Self-Assembling of Zinc Phthalocyanines on ZnO ($10\bar{1}0$) Surface through Multiple Time Scales

Claudio Melis,[†,‡,*] Paolo Raiteri,[§] Luciano Colombo,[†,‡] and Alessandro Mattoni[‡]

[†]Dipartimento di Fisica, Università di Cagliari, I-09042 Monserrato (Ca), Italy, [‡]Istituto Officina dei Materiali del CNR UOS Cagliari, I-09042 Monserrato (Ca), Italy, and [§]Nanochemistry Research Institute, Department of Chemistry, Curtin University, P.O. Box U1987, Perth, WA 6845, Australia

ABSTRACT

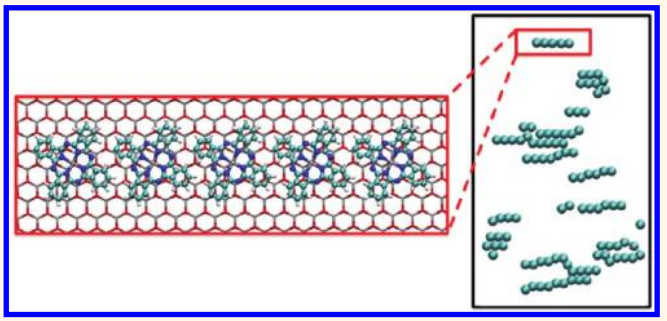

We adopt a hierarchic combination of theoretical methods to study the assembling of zinc phthalocyanines (ZnPcs) on a ZnO ($10\bar{1}0$) surface through multiple time scales. Atomistic simulations, such as model potential molecular dynamics and metadynamics, are used to study the energetics and short time evolution (up to ~100 ns) of small ZnPc aggregates. The stability and the lifetime of large clusters is then studied by means of an atomistically informed coarse-grained model using classical molecular dynamics. Finally, the macroscopic time scale clustering phenomenon is studied by Metropolis Monte Carlo algorithms as a function of temperature and surface coverage. We provide evidence that at room temperature the aggregation is likely to occur at sufficiently high coverage, and we characterize the nature, morphology, and lifetime of ZnPc's clusters. We identify the molecular stripes oriented along [010] crystallographic directions as the most energetically stable aggregates.

KEYWORDS: hybrid interface · free energy · self assembling · multiscale modeling · phthalocyanines

Hybrid heterostructures consisting of metal oxides functionalized by metallo-organic macrocyclic complexes (MOMC) have attracted large interest for photoelectrochemical and photocatalysis applications as well as for low-cost photovoltaics (*e.g.*, dye-sensitized solar cells).[1−4] In photovoltaic devices, the role of the organic MOMCs is to absorb light (dye) and to donate electrons to the metal oxide while collecting holes.[5] Among MOMCs, phthalocyanines (Pcs) are widely used as dye molecules, and they represent a cheap and environmentally friendly alternative to pyridyl-based compounds.[6] Pcs are characterized by an intensive absorption in the far-red IR region, together with excellent chemical, light, and thermal stability.[6] The structure of these molecules is characterized by one or more macrocyclic ligands carrying clouds of delocalized electrons and by a central metal or group. Almost all of the metals appearing in the periodic table can be used to synthesize Pc molecules, differing in their spectroscopic and electrochemical properties.[7]

As for the inorganic component, wide band gap metal oxides (*e.g.*, ZnO, TiO_2) are used as efficient electron acceptors characterized by a strong photoanodic stability against degradation[8] and a low rate of direct electron−hole recombination processes.[3] TiO_2 was the first metal oxide anode for which efficient visible sensitizations by MOMCs was observed.[9] It is still the most widely adopted material for hybrid photovoltaic applications. In recent years, ZnO has rapidly emerged as a valid alternative to titania since it can be synthetized with great flexibility, it is nontoxic, and it provides very good electron mobility.[10]

In this work, we focus on the case of ZnPc/ZnO hybrids. These systems, showing sizable photocurrents, have been used as active interfaces for photovoltaics (both with electrolytes or in solid state systems). The photophysics of ZnO functionalized by ZnPcs is affected by temperature, molecular concentration, and the ZnO surface morphology.[11,12] These effects are mostly related to the tendency of Pcs to aggregate at the interface.[12] In fact, aggregation can easily occur during synthesis in solution or in the gas phase,[13] as well as a result of thermally activated molecule diffusion on the metal oxide surface.[14] It has been shown that Pc aggregates have electrochemical, spectroscopic, photophysical, and

* Address correspondence to claudio.melis@dsf.unica.it.

Received for review August 13, 2011 and accepted November 2, 2011.

Published online November 02, 2011
10.1021/nn203105w

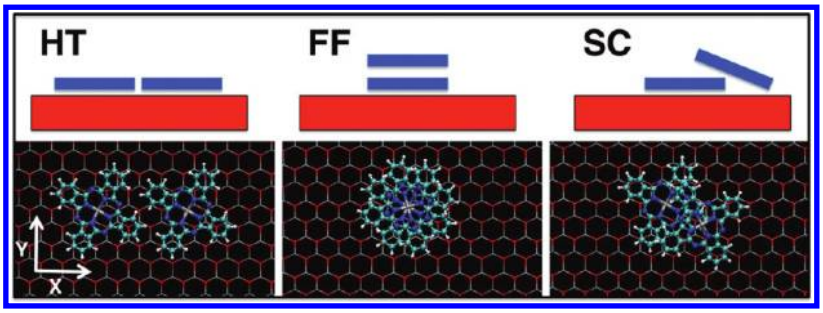

Figure 1. Ball-and-stick representation of the ZnPc dimer/ZnO bound states. Left: head-to-tail configuration. Middle: face-to-face configuration. Right: slipped cofacial configuration. The side views of these configurations are sketched in the top panel.

conductive properties different from those of the corresponding monomers. In particular, aggregation turns out to be detrimental for charge transfer and results in a strong decrease of the quantum efficiency.[7] Two kinds of aggregates have been identified according to their optical absorption properties: (i) H-type, where the molecules are parallel according to a face-to-face (FF, schematically represented in top middle panel of Figure 1) or a slipped cofacial alignment (SC, top right); (ii) J-type aggregates, where the molecules are parallel according to a head-to-tail (HT, top left) alignment. J-type (H-type) aggregates give rise to red (blue) shift transitions in the absorption spectra with respect to the monomer.[13]

In ref 11, the absorption spectrum of the ZnPc/ZnO surface has been measured. Absorption bands that occur at wavelengths greater than 750 nm are attributed to molecular aggregates on the surface. By resonance light scattering measurements, it was found that aggregation on the surface increases with the ZnPc concentration. The effect of thermal treatment on ZnPc/ZnO hybrids was studied, as well.[11] A strong improvement of the photocurrent by annealing in the 150−350 °C range of temperatures was observed. A clear explanation for this observation is missing, and it is most likely related to thermal effects on aggregation.

In the present work, the energetics and the dynamics of ZnPc molecules on the ZnO surface are studied. In particular, we focus on ZnPc molecules adsorbed on a planar wurtzite ZnO nonpolar $(10\bar{1}0)$ surface, which is the most favorable wurtzite ZnO surface. As discussed elsewhere,[14] it was found that ZnPcs are adsorbed on the three-coordinated oxygens on the surface and diffuse on the surface at room temperature. Here, we extend the above analysis by focusing on aggregation phenomena. The molecular aggregation phenomena occur at different time and size scales with respect to the atomic ones (femtoseconds and nanometers), controlling mobility and molecule−molecule interaction, up to milliseconds and micrometers where molecular collective motions occur. Accordingly, here we adopt a hierarchic combination of theoretical methods: atomistic simulations, model potential molecular dynamics (MPMD), and metadynamics are used to study the energetics and the short time evolution (up to ∼1 μs) of small ZnPc dimers. The atomistic results are then used to obtain a coarse-grained model (CGM) describing the molecule−surface and molecule−molecule effective interactions. By molecular dynamics based on CGM, we study the evolution of large molecular aggregates in the microsecond scale. Metropolis Monte Carlo is further adopted to extend the time scale by studying the equilibrium distribution of large aggregates (in the micrometer length scale) as a function of temperature and coverage.

RESULTS AND DISCUSSION

We study the assembling of ZnPcs *via* multiple time and size scale analyses. The first section describes the energetics and the short time scale (∼100 ns) dynamics of ZnPc dimers described at the atomistic level. The second section describes the energetics and the intermediate time scale (∼μs) dynamics of larger aggregates, and it is obtained by using the coarse-grained model. In the last section, we report the long time scale (∼ms) evolution of large molecular aggregates as a function of temperature and surface coverage.

Energetics and Short Time Scale Dynamics of ZnPc Dimers. The ZnPc adsorption on the ZnO $(10\bar{1}0)$ surface was studied in ref 14. It was found that the molecule is adsorbed on sites corresponding to the surface three-coordinated oxygens with 2.2 eV adsorption energy. Two energetically equivalent orientations of the molecule on the site were found, named *A*, *A*′ plus a third *B* orientation slightly larger in energy.

In order to study the energetics of aggregation, we consider first the case of molecule dimers of type FF and HT that are the building block of larger aggregates. As for the HT dimer, we performed an extensive analysis of the configurational space of two adsorbed ZnPcs both facing the ZnO surface. In particular, we placed one molecule on the *A* configuration, and we varied the position of the second molecule over sites in a circular region within radial distances of 12−25 Å. At each site, we considered different orientations of the second molecule around the center of mass. For each

possibility, we fully relaxed the system and calculated the total energy in order to find the minimum energy configurations. The lowest energy dimer is the *AA* (Figure 1, left panel). In the *AA* configuration, two molecules in the *A* orientation are shifted along the [010] direction by a distance of 13.6 Å ($\sim 4a$, where $a = 3.35$ Å is the ZnO surface lattice constant along the *X* direction). In this configuration, the two molecules are locked together (see left panel Figure 1) with a lateral interaction as small as ~0.1 eV. A symmetric configuration $A'A'$ is found as well where the two molecules are in the A' orientation.

We also investigate the FF dimers. Starting from one of the two molecules adsorbed on the surface in the *A* configuration, we stacked the second molecule over the first one at different distances within the range of 2.5−14 Å . For each distance, we considered different rotated positions of the second molecule, and we relaxed the atomic forces and positions. The most stable FF configuration (see middle panel Figure 1) is found for a distance of 3.83 Å and a relative rotation of $\sim\pi/4$ such that the benzene rings are not overlapped. The geometry of the top molecule is close to the ideal planar geometry, indicating only a partial interaction with the surface. Distortions induced by the surface are observed only on the first molecule. The adsorption energy of the second molecule is 1.86 eV (*i.e.*, 0.34 eV lower than the adsorption energy of an isolated ZnPc on the surface).

The better stability of the HT dimer geometry is explained by the fact that the molecule−substrate adhesion (2.2 eV) is larger than the molecule−molecule binding (1.6 eV). This latter result is in agreement with previous findings.[15] Therefore, the adsorption of ZnPc molecules on the ZnO $(10\bar{1}0)$ surface is favored with respect to their stacking, and the formation of ZnPc monolayers is energetically favored.

A further interesting feature is the occurrence of an intermediate geometry (see right panel of Figure 1) between FF and HT configurations. This dimer has a binding energy of 1.5 eV, having the first molecule adsorbed on the surface in the *A* geometry and the second one slipped cofacial (SC) and rotated by $\theta \sim \pi/12$. The Zn−Zn distance of the two molecules is 7 Å. The SC dimer is energetically unfavored with respect to HT by ~0.7 eV.

FF dimers are relevant since they can occur during synthesis of ZnPc/ZnO layers. Dimers of stacked molecules can, in fact, easily form in solution[11] or in the gas phase[15] and eventually be adsorbed on the ZnO surface as FF dimers. Since they are energetically unfavored, they can further evolve at room temperature into the lower energy HT configuration by overcoming a free energy barrier. The height of this barrier controls the FF lifetime and the relative population of dimers. Therefore, it is important to estimate the paths and the barriers separating the different ZnPc dimers. To this

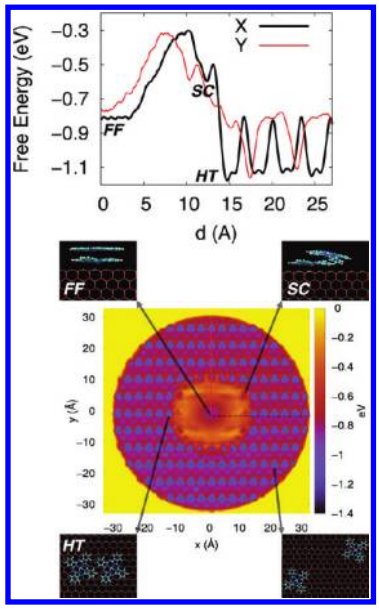

Figure 2. Bottom: Color map of the interaction free energy of two ZnPCs adsorbed on the ZnO $(10\bar{1}0)$ surface (see text for details). The minima (dark blue) corresponds to the molecule adsorption sites. The yellow region corresponds to a portion of the CV space which was not explored. All of the geometries found previously (FF, HT, and SC) have been explored by the metadynamics and are shown in the panels; the arrows indicate the position on the 2D free energy profile. Top: Energy profiles calculated along the two directions *X* and *Y* reported in the bottom panel as dotted lines.

aim, we make use of metadynamics choosing as collective variables the *x* and *y* position of one molecule center of mass on the ZnO $(10\bar{1}0)$ surface and restraining the other molecule to remain in the central adsorption site. Figure 2 (bottom panel) shows the corresponding free energy map, while the top panel shows the free energy profiles along the *X* and *Y* directions. The 2D free energy profile in Figure 2 clearly shows deep minima corresponding to the various adsorption sites for the second ZnPc while there is a high energy region in the center of the plot which corresponds to the FF and SC configurations. In order to have a more quantitative understanding of the energetics of the ZnPc pairing, we looked at the free energy profile along the *X* and *Y* directions (Figure 2, top panel). The free energy profile calculated from the metadynamics confirms the presence of all the configurations found before (FF, HT, and SC) and their stability trend. The FF dimer can transform into the SC configuration by overcoming an energy barrier of ~0.4 eV with a marginal energy gain and subsequently by overcoming a smaller energy barrier (~0.2 eV) to the HT configuration that is about 0.3 eV lower in energy and located at $X \sim 15$ Å. The minima along *X* and *Y* have different spacing due to the asymmetry of the adsorption sites along the two directions, but it is clearly evident that when the molecules are sufficiently far apart their interaction is very weak and the diffusion will be limited by the rate of escape from the

adsorption site. In the regime of very large distances, an important contribution to the free energy is given by the configurational entropy which constantly lowers the free energy as $-k_BT\ln(R)$. This term, which is naturally included in MD simulations, would appear if a radial average were taken. However, this contribution is not evident in the cross sections of the 2D free energy profiles along *X* and *Y* reported in Figure 2. By going from 15 to 30 Å, this contribution decreases the free energy by an amount as small as 18 meV. This implies that at very low coverage the thermodynamically stable configuration will correspond to the ZnPcs dispersed on the ZnO surface. Quantitatively, this term contributes for about k_BT when the distance between the ZnPcs increases from 10 to 30 Å. In the Theoretical Framework section at the end of the article, we show that the ZnPcs have an attractive interaction of about 0.1 eV at 14 Å. In the free energy profile (Figure 2, top panel), there are two entropic contributions which partially compensate the attractive term. These are namely the entropic terms related to the fact the ZnPcs are no longer locked into a fixed relative orientation at that distance and one related to change in the internal vibrational modes. At this stage, it is hard to accurately calculate the magnitude of these contributions, but we can reasonably expect them to be on the order of $2-3\ k_BT$.

Present metadynamics calculations have been performed in a regime of low coverage (two ZnPc molecules adsorbed on a surface as large as 7×8 nm^2, roughly corresponding to a coverage of 0.035 monolayers, ML). *R* can span a range of distances as large as 0.3 nm, and in agreement with the above discussion, we find that the global minimum corresponds to separated molecules. We define the surface coverage ρ as the surface area occupied by the molecules (A_Mn) divided by the total surface area (*S*): $\rho = A_Mn/S$, where A_Mn is equal to the total number of adsorbed molecules *n* multiplied by the area of each molecule A_M (~150 Å^2 for ZnPc). The average intermolecular distance *R* depends on the coverage according to $R \sim \rho^{-0.5}$. Therefore, by varying the surface coverage, it is possible to tune the global minimum of the free energy. For low coverages, the free energy global minimum corresponds to the two separated molecules. At medium coverages, the minimum corresponds to the HT configuration, and at higher coverages, the minimum is the FF configuration.

Energetics and Intermediate Time Scale Dynamics of Larger ZnPcs Aggregates: Molecular Stripes. According the results of the previous section, the formation of ZnPc dimers on the ZnO surface is expected at high coverages. Here, we study the formation of larger aggregates by assembling up to five molecules. In particular, we compare the energetics of H-type aggregates (hereafter named FF*n*, where *n* is the number of molecules) or J-type aggregates (HT*n*). In order to identify the morphology

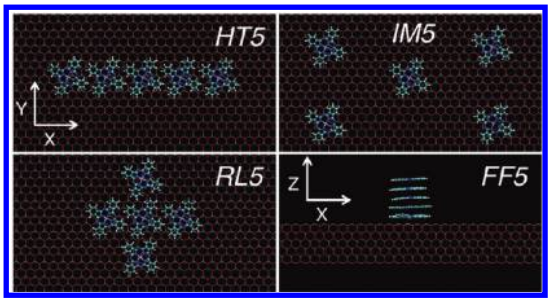

Figure 3. Ball-and-stick representation of the most energetically stable configurations of five ZnPcs.

of the aggregates, we adopt a similar procedure described for the search of dimers with an extensive exploration of the configurational space. Figure 3 shows the stable configurations identified within present analysis.

We consider first an H-type aggregate obtained by successively stacking up to five molecules bound together *via* $\pi-\pi$ and electrostatic interactions (Figure 3, bottom right). The adsorption energy of the last top molecule is calculated as a function of the number of stacked molecules. From the third to the fifth molecule, we always find almost the same absorption energy (~1.9 eV), which is smaller than the molecule adsorption energy on the surface (2.2 eV). This confirms that dimers tend to bind to the surface rather than growing in the gas phase.

As for J-type aggregates, we consider stripes formed by up to five molecules (Figure 3, top left) oriented along the [010] direction. All of the molecules are locked together at a distance of ~13.6 Å, with attractive interactions. This HT5 aggregate is 1.7 eV more stable than the FF5. This result confirms the tendncy of the molecule to create monolayers on the surface rather than multilayers. For another aggregate, we considered round-like structure (RL5) (Figure 3, bottom left), involving the locking of the molecules both in the *X* and *Y* directions. This cluster has been already proposed for metallic substrates[16,17] or in the case of graphene.[18] This RL configuration is energetically unfavored with respect to the HT5 linear stripes by 1.0 eV. This is due to the different periodicity of the surface along the *Y* direction that hardly matches the molecule−molecule equilibrium distance.

Finally, we consider the case of isolated molecules IM5 (Figure 3, top right) adsorbed on the surface. This case is energetically favored with respect to RL5 by 0.6 eV. In summary, we found that the most stable aggregate is HT5, followed by IM5 (+0.4 eV), RL5 (+1.0 eV), and FF5 (+1.7 eV). In conclusion, multilayered stacks are always unfavored with respect to monolayer aggregates. Within these latter instances, the linear stripes are the most stable.

According to present analysis, we identify the observed J-like aggregates as linear stripes along the [010] direction. Similar types of aggregates have been experimentally

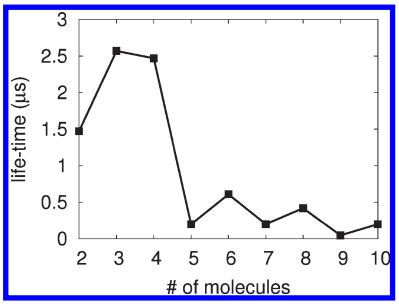

Figure 4. Stripe lifetime as a function of their length (number of beads).

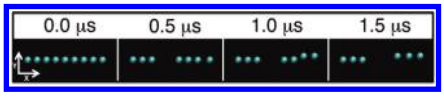

Figure 5. Time evolution of a stripe formed by nine beads evolving in shorter stripes before dissolving.

identified in the case of CuPc/TiO_2 hybrids.[19] It is reasonable to conclude that the observed absorption bands at wavelengths greater than 750 nm in ZnPc/ZnO hybrids[11] are related to such kinds of aggregates.

As previously done in the case of dimers, we study the dynamical behavior of stripes at room temperature. In order to limit the computational cost and to extend the time and length scales, we adopt a different procedure rather than atomistic metadynamics. We adopt a coarse-grained model (see Theoretical Framework section) in which each ZnPc is represented as a bead interacting, through suitable effective potentials, with other molecules and the surface. In this way, we are able to calculate the trajectories of aggregates over a microsecond time scale and, in particular, the time evolution and lifetime of stripes of different lengths.

We adopt a velocity Verlet algorithm with time step of 0.1 fs to numerical integration of trajectories and a Langevin thermostat to fix T = 300 K. We consider stripes formed by up to 10 beads. In all cases, isolated stripes dissociate in the microsecond time scale.

We define that lifetime τ of a stripe as the time necessary to have the first dissolution event. Lifetimes (Figure 4) are calculated as the average of five different simulations at different temperatures (298−302 K). The error bars, corresponding to the maximum deviation from the average, are within the size of the symbols. We find that τ depends on the stripe size (see Figure 4). The stripes formed by three and four elements are the most stable at room temperatures with lifetimes in the order of ∼2.5 μs. Long stripes are less stable with lifetimes of ∼0.1−0.5 μs.

An example of dissolution is reported for a nine-bead stripe. The stripe breaks into two pieces that in turn further dissolves up to the formation of isolated molecules (Figure 5).

In conclusion, at room temperature and in a regime of low coverage, the large aggregates dissolve into isolated molecules. This is consistent with metadynamics results for dimers. The above scenario can change when increasing the coverage, and it is the object of the next section.

Long Time Scale Dynamics of Large ZnPc Aggregates: Clustering as a Function of Temperature and Coverage. The calculation of the dynamical behavior of aggregates in the case of hundreds of molecules is computationally expensive if we adopt the same procedure discussed above. Since we are interested in the population of aggregates at equilibrium under different conditions of coverages, we here adopt a Metropolis Monte Carlo protocol as a more computationally efficient alternative. The Monte Carlo move consists of a single bead (randomly chosen) that hops between neighboring adsorption sites. The acceptance is controlled by the Metropolis algorithm according to the change in the configurational energy. The energy is calculated by using the effective intermolecular potential already described. We consider always a number of beads as large as 100, and we chose surfaces of different area giving the coverage of interest. Two molecules are aggregated when their distance is <18 Å. We performed 10^8 steps for each Monte Carlo run, and we sampled the configurations during the last 30 million steps once equilibrium was achieved.

The quantity of interest in this study is the relative cluster distribution function (RCDF). RCDF is defined as follows: first we calculate the number of molecules belonging to aggregates of size s (cluster distribution function cdf(s)). Then we consider the function cd0(s) corresponding to a random distribution of molecules at the same coverage. RCDF is finally defined as RCDF(s) = cdf(s) − cd0(s). Cdf and cd0 are both positively defined, while RCDF can be negative if cdf < cd0. Positive (negative) values of RCDF(s) represent an increased (decreased) number of aggregates with respect to random distribution. For example, for the case of T = 200 K and ρ = 0.2 ML (see Figure 7), as a result of aggregation, the number of isolated molecules cdf(1) is lower that in the random case cd0(1). Accordingly, RCDF(1) is negative.

We study different values of coverage (ρ = 0.05, 0.1, 0.2, 0.3, 0.4, 0.5 ML). Figure 6 shows examples of snapshots at different ρ. We found that the number of aggregated molecules increases with ρ. In particular, more than 50% of the molecules are aggregated at ρ > 0.2 ML. This value of coverage is defined as the threshold coverage for the molecule aggregation. Most of the clusters are stripes oriented along the [010] direction.

The analyses based on RCDF are reported in Figure 6 and show a decrease in the number of monomers with respect to the random distribution. At ρ = 0.4 and 0.5 ML, most of the molecules are aggregated even in the random distribution. Intermolecular interactions further increase the number of large aggregates (s > 80; see Figure 6, right bottom panel). When ρ < 0.2 ML, the fraction of aggregated molecule is below 50%. In this case, the clusters are mainly short stripes (formed by 2, 3, 4, and 5 elements). At coverages greater than 0.2 ML, the fraction of assembled

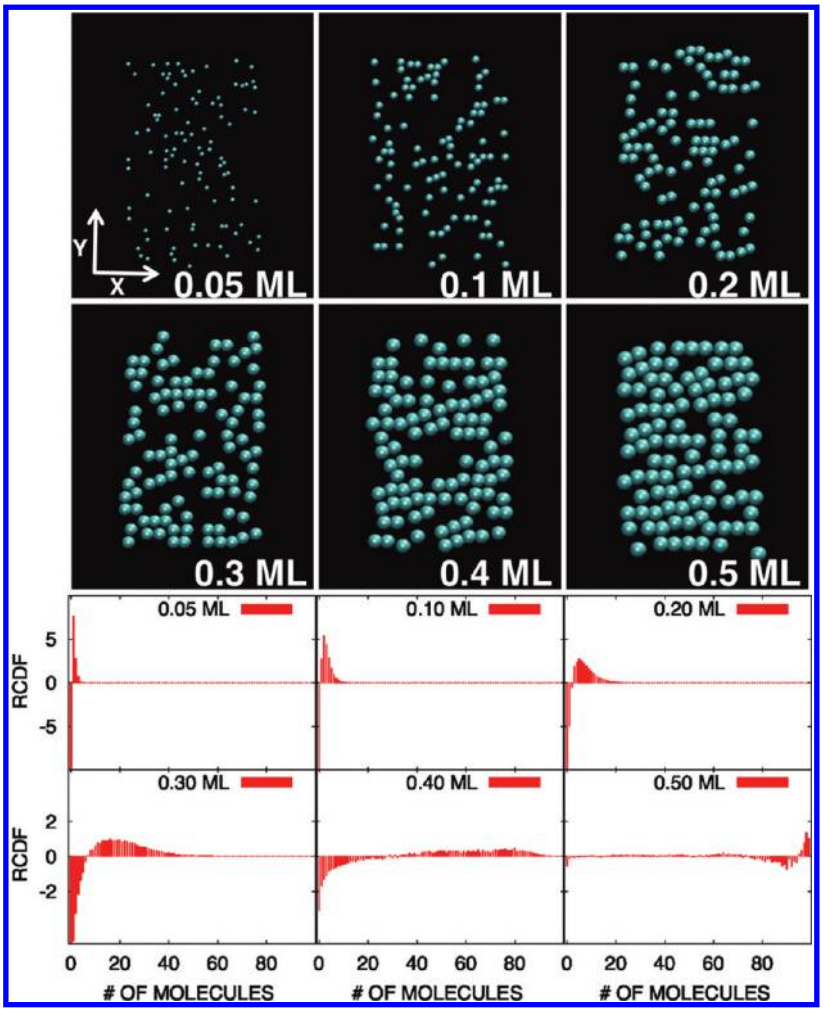

Figure 6. Top: final snapshots of the Metropolis Monte Carlo simulations performed at fixed temperature (T = 300 K) and different surface coverages (0.05−0.5 ML). Relative cluster distribution function (RCDF) at fixed temperature (T = 300 K) and different surface coverages (0.05−0.5 ML) as a function of the cluster dimensions (number of molecules).

molecules strongly increases (61% at 0.3 ML, 72% at 0.4 ML, and 80% at 0.5 ML), forming stripes of different dimensions (up to 10 beads). This analysis shows that a sizable effect of aggregation must be expected at coverage >0.2 ML.

We are able to extend the present analysis to take into account the effect of temperature. Results are shown in Figure 7 (right) for the fixed threshold coverage ρ = 0.2 ML. The general trend is that by lowering the temperature the stripes tend to be larger. By studying the RCDF, we always find a decrease of isolated molecules indicating aggregation. However, we observe differences between the low-temperature and high-temperature regimes. At 100 K, the population shows a trimodal distribution in which small (∼10 beads), medium (∼30 beads), and larger clusters (∼40 beads) are present. The occurrence of such a trimodal distribution is explained by the fact that at 100 K the molecular stripes, whose average length is ∼10 beads, tend to aggregate, forming larger clusters having a length in multiples of 10 beads. At such a low temperature, by hugely increasing the number of Monte Carlo steps, we expect that all of the molecules tend to aggregate, forming a single 100 bead cluster. Below 200 K, most of the molecules are aggregated (98% at 100 K, 74% at 200 K). Above 200 K, the fraction of assembled molecules decreases down to 50% (52% at 300 K, 35% at 400 K, 28% at 500 K, 24% at 600 K). We observe an exponential decrease of the fraction of aggregated beads with the temperature. From the corresponding Arrhenius plot, we calculate an activation energy E_A = 0.05 eV for the cluster dissolution, which is comparable to the intermolecular binding energy energy (0.1 eV).

The exponential decrease of clustering is consistent with experiments, indicating an improvement of the photocurrent with temperature. Since the aggregations are detrimental for photocurrent (by reducing absorption and charge transfer), the temperature by dissolving clusters is expected to be beneficial for the system.

The fundamental role of temperature and coverage on aggregation is confirmed by the experiments, showing that the optoelectronic properties of the ZnPc/ZnO hybrid strongly depends on both temperature and surface coverage.[11]

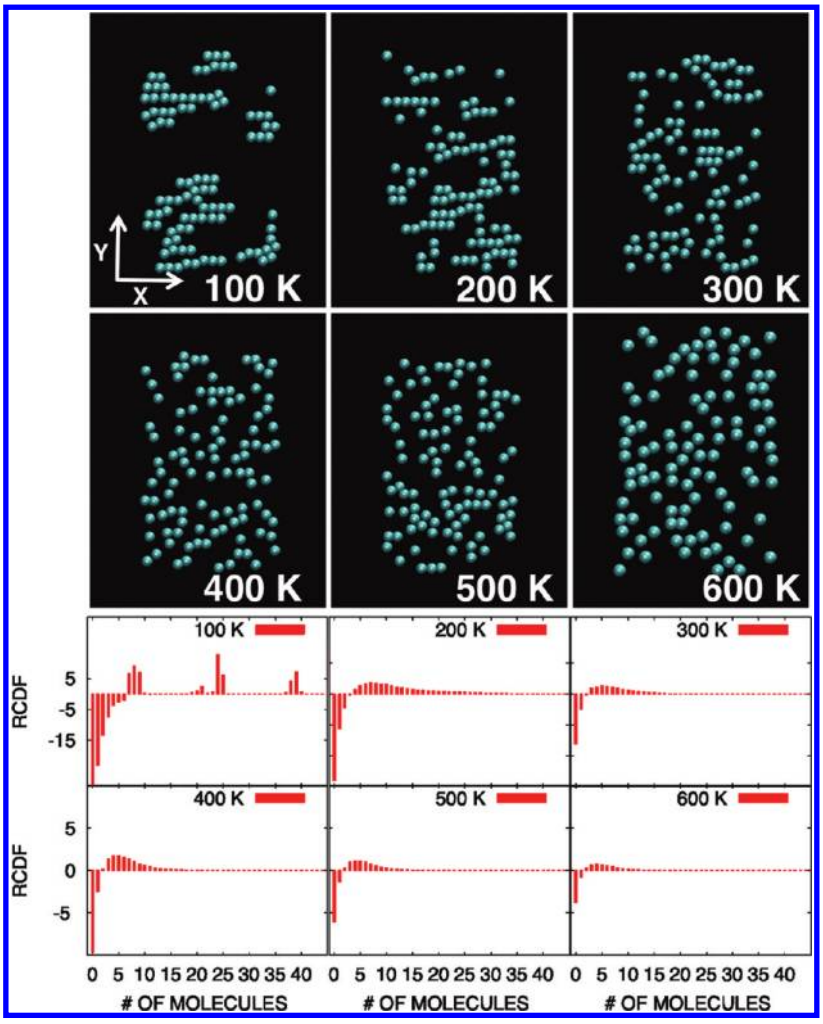

Figure 7. Top: Final snapshots of the Metropolis Monte Carlo simulations performed at fixed coverage (ρ= 0.2) and different temperatures (100−600 K). Bottom: RCDF at fixed coverage (ρ = 0.2) and different temperatures (100−600 K) as a function of the cluster dimensions.

CONCLUSIONS

In conclusion, we successfully adopted a hierarchic combination of theoretical methods to study the assembling of zinc phthalocyanines (ZnPcs) on a ZnO $(10\bar{1}0)$ surface through multiple time scales. Atomistic simulations, such as model potential molecular dynamics and metadynamics, are used to study the energetics and short time evolution (up to $\sim 10^2$ ns) of small ZnPcs aggregates. We identify molecular stripes oriented along the [010] crystallographic directions as the most energetically stable aggregates. We provide evidence that at room temperature the lifetime of dimers and small molecular stripes is as short as a few microseconds. However, above 0.2 ML coverage, the aggregation involves more than 50% of molecules.

THEORETICAL FRAMEWORK

The atomistic calculations have been performed by MPMD by combining existing force fields for ZnO and ZnPc and by adding long-range Coulomb and dispersive interactions to model interactions across the ZnO/ZnPc interface. The interatomic potential for ZnO wurtzite is described by the sum of a Coulomb and a Buckingham-type two-body potential,[20,21] which have been successfully applied[22] to study nanostructured ZnO. The parameters for ZnO were taken from ref 23. In order to describe ZnPc, we used the AMBER force field[24] that includes either bonding (streching, bending, torsional) and nonbonding (van der Waals plus Coulomb) contributions. The ZnPc atomic partial charges have been estimated by DFT calculations with the electrostatic potential (ESP[25]) procedure using the CPMD code.[26] Interatomic forces between atoms of the ZnPc and the ZnO substrate were calculated by including electrostatic and dispersive interactions. Coulomb terms involved interactions between atomic partial charges of the molecule and the ZnO ions. Dispersive interactions of the Lennard-Jones type were taken from the AMBER database.[24] The reliability of the present force model has been discussed in ref 14, where the adhesion energy and the diffusion of a single ZnPc molecule on the ZnO substrate was studied in detail.

The atomistic simulations were performed by using DL_POLY[27] (version 3). Atomic trajectories were calculated by using the velocity Verlet integrator, with a time step as small as 1.0 fs. Long-range electrostatic forces were evaluated using a particle mesh Ewald algorithm.[28] A cutoff as large as 9.5 Å was used in order to accurately calculate the van der Waals interactions. The simulation protocol used for geometry optimization consisted of a combination of 0.1 ns low-temperature molecular dynamics followed by conjugate gradients.

The assembling of two ZnPcs at room temperature was studied by using the metadynamics technique, which allows one to accelerate rare events and to sample the free energy as a function of suitable collective variables.[29] Metadynamics works by adding a history-dependent potential, built as a sum of Gaussians, whose role is to discourage the system from revisiting regions already visited, thus accelerating barrier crossings. We used as collective variables the x and y position of one molecule center of mass on the ZnO $(10\bar{1}0)$ surface and restraining the other molecule with a quartic potential to the central adsorption site. The quartic potential was chosen so that its effect was minimal in the absorption site and strong outside to prevent the ZnPc escape. The simulations were performed at 300 K and for a total time of 1.2 μs. In order to accelerate the exploration of the CV space and convergence, we employed the multiple walkers[30] (456 walkers) and well-tempered[31] (bias factor = 15) schemes. The Gaussians had a width of 0.1 Å and were deposited at intervals of 0.5 ps. The initial height of the Gaussians was 0.026 eV, and at the end of the simulation, it was always smaller than 0.001 eV. In order to limit the size of the CV space to be explored, we also restrained the ZnPcs to be within 30 Å from each other. This effectively limits the reliability of the calculated 2D free energy profile to a distance of about 27 Å from the central one.

In order to study the stability of the ZnPc aggregates as well as their assembling as a function of coverage and temperature, we adopt a coarse-grained approach to model the effective molecule−surface and molecule−molecule interaction potentials. In this scheme, each ZnPc is described as a bead (with only two translational degrees of freedom) that interacts with the lattice and the other molecules *via* effective potentials. This approach extends the simulated time scale up to the micro/milliseconds and length scales up micrometers, making possible a comparison with the experiments.

The effective molecule−surface interaction is obtained by metadynamics. In particular, the free energy of a molecule−surface system is calculated as a function of the position of the molecule on the surface.[14]

The effective molecule−molecule interaction is calculated by keeping two molecules frozen in the absorbed geometry and orientation and by varying their relative position. We fix one molecule in the origin (Figure 8), and we shift the second one at different $X-Y$ positions (-30 Å $< X <$ 30 Å, -30 Å $< Y <$ 30 Å) by steps of 0.1 Å (3.6×10^5 points). At each point, the energy is calculated by an atomistic model potential by using the DL_POLY code. In Figure 8 (bottom), the two molecules (one placed at 0,0 and the second one at a generic $X-Y$ position) are reported as ball-and-stick on the color map. The three curves in Figure 8 (top panel) are the interaction energy calculated moving the second molecule along the three directions A ($X-Y$ bisector), B (X axis), and C (Y axis) reported in the bottom panel. It is found that the interaction is short-range with a strong dependence on the intermolecular orientation (see Figure 8, top). The largest attraction energy is ~0.1 eV, giving rise to eight symmetric minima at a distance of about 1.4 nm.

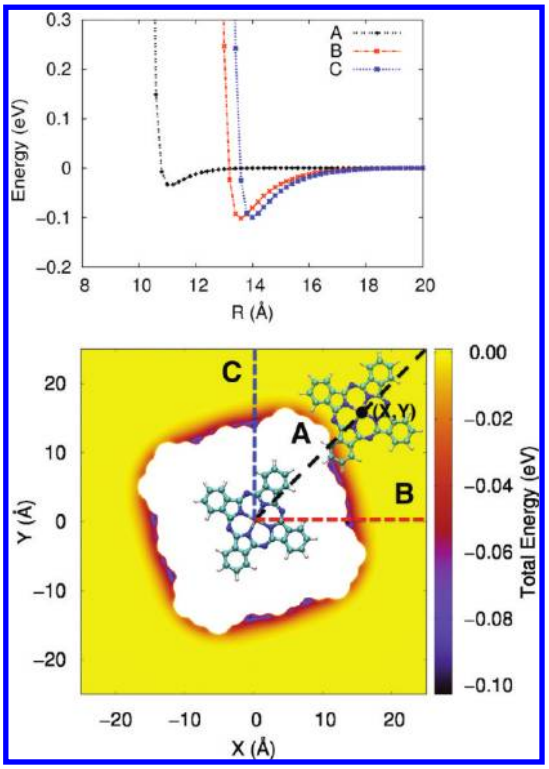

Figure 8. Bottom: Color map of the molecule−molecule interaction energy of two ZnPcs as a function of their relative position (X, Y). White color corresponds to repulsive interactions so intense to result out of scale with respect to the color scale reported on the right. Attractive interactions (E < 0 eV, dark blue-orange colors) gives rise to eight symmetric minima at intermolecular distances of about 1.4 nm. Yellow regions correspond to noninteracting molecules. Top: Energy profiles calculated along the three directions A ($X-Y$ bisector), B (X axis), and C (Y axis) reported in the bottom panel as dotted lines.

Acknowledgment. We acknowledge computational support by CYBERSAR (Cagliari, Italy), CINECA (Casalecchio di Reno, Italy; Grant IscrA_SIMuLATe), and CASPUR (Rome, Italy) and Italian Institute of Technology (IIT) under Project SEED "POLYPHEMO". P.R. thanks the Australian Research Council for funding through the Discovery Grant program (DP0986999), IVEC and NCI for providing computational resources, as well as the Visiting

Professorship program of Regione Sardegna for having prompted this collaboration.

REFERENCES AND NOTES

1. Forrest, S. R. Ultrathin Organic Films Grown by Organic Molecular Beam Deposition and Related Techniques. *Chem. Rev.* **1997**, *97*, 1793–1896.
2. Nelson, J. Organic Photovoltaic Films. *Curr. Opin. Solid State Mater. Sci.* **2002**, *6*, 87–95.
3. Grätzel, M. Conversion of Sunlight to Electric Power by Nanocrystalline Dye-Sensitized Solar Cells. *J. Photochem. Photobiol. A* **2004**, *164*, 3–14.
4. Mattioli, G.; Filippone, F.; Giannozzi, P.; Caminiti, R.; Amore Bonapasta, A. Theoretical Design of Coupled Organic–Inorganic Systems. *Phys. Rev. Lett.* **2008**, *101*, 126805–126808.
5. Hagfeldt, A.; Grätzel, M. Light-Induced Redox Reactions in Nanocrystalline Systems. *Chem. Rev.* **1995**, *95*, 49–68.
6. Hains, A. W.; Liang, Z.; Woodhouse, M. A.; Gregg, B. A. Molecular Semiconductors in Organic Photovoltaic Cells. *Chem. Rev.* **2010**, *110*, 6689–6735.
7. He, J.; Benkö, G.; Korodi, F.; Polvka, T.; Lomoth, R.; Åkermark, B.; Sun, L.; Hagfeldt, A.; Sundström, V. Modified Phthalocyanines for Efficient Near-IR Sensitization of Nanostructured TiO_2 Electrode. *J. Am. Chem. Soc.* **2002**, *124*, 4922–4932.
8. Reutergardh, L. B.; Iangphasuk, M. Photocatalytic Decolourization of Reactive Azo Dye: A Comparison between TiO_2 and CdS Photocatalytis. *Chemosphere* **1999**, *35*, 585–596.
9. Reddy, P. Y.; Giribabu, L.; Lyness, C.; Snaith, H. J.; Vijaykumar, C.; Chandrasekharam, M.; Lakshmikantam, M.; Yum, J. H.; Kalyanasundaram, K.; Grätzel, M.; *et al.* Efficient Sensitization of Nanocrystalline TiO_2 Films by a Near-IR-Absorbing Unsymmetrical Zinc Phthalocyanine. *Angew. Chem., Int. Ed.* **2007**, *46*, 373–376.
10. Özgür, U.; Alivov, Y. I.; Liu, C.; Teke, A.; Reshchikov, M. A.; Doğan, S.; Avrutin, V.; Cho, S.-J.; Morkoç, H. A Comprehensive Review of ZnO Materials and Devices. *J. Appl. Phys.* **2005**, *98*, 041301–041404.
11. Ingrosso, C.; Petrella, A.; Cosma, P.; Curri, M. L.; Striccoli, M.; Agostiano, A. Hybrid Junctions of Zinc (II) and Magnesium (II) Phthalocyanine with Wide-Band-Gap Semiconductor Nano-Oxides: Spectroscopic and Photoelectrochemical Characterization. *J. Phys. Chem. B* **2006**, *110*, 24424–24432.
12. Ingrosso, C.; Petrella, A.; Curri, M.; Striccoli, M.; Cosma, P.; Cozzoli, P.; Agostiano, A. Photoelectrochemical Properties of Hybrid Junctions Based on Zinc Phthalocyanine and Semiconducting Colloidal Nanocrystals. *Electrochim. Acta* **2006**, *51*, 5120–5124.
13. Zhang, X.; Xi, Q.; Zhao, J. Fluorescent and Triplet State Photoactive J-Type Phthalocyanine Nano Assemblies: Controlled Formation and Photosensitizing Properties. *J. Mater. Chem.* **2010**, *20*, 6726–6733.
14. Melis, C.; Colombo, L.; Mattoni, A. Adhesion and Diffusion of Zinc-Phthalocyanines on the ZnO $(10\bar{1}0)$ Surface. *J. Phys. Chem. C* **2011**, *115*, 18208–18212.
15. Marom, N.; Tkatchenko, A.; Scheffler, M.; Kronik, L. Describing Both Dispersion Interactions and Electronic Structure Using Density Functional Theory: The Case of Metal-Phthalocyanine Dimers. *J. Chem. Theory Comput.* **2010**, *6*, 81–90.
16. Chau, L.-K; Arbour, C.; Collins, G.; Nebesny, K. W.; Lee, P. A.; England, C. D.; Armstrong, N. R.; Parkinson, B. A. Phthalocyanine Aggregates on Metal Dichalcogenide Surfaces: Dye Sensitization on Tin Disulfide Semiconductor Electrodes by Ordered and Disordered Chloroindium Phthalocyanine Thin Films. *J. Phys. Chem.* **1993**, *97*, 2690–2698.
17. Cheng, Z. H.; Gao, L.; Deng, Z. T.; Jiang, N.; Q. Liu, D. X. S.; Du, S. X.; Guo, H. M.; Gao, H.-J. Adsorption Behavior of Iron Phthalocyanine on Au(111) Surface at Submonolayer Coverage. *J. Phys. Chem. C* **2007**, *26*, 9240–9244.
18. Wang, S. D.; Dong, X.; Lee, C. S.; Lee, S. T. Orderly Growth of Copper Phthalocyanine on Highly Oriented Pyrolytic Graphite (HOPG) at High Substrate Temperatures. *J. Phys. Chem. B* **2004**, *108*, 1529–1532.
19. Wang, Y.; Ye, Y.; Wu, K. Adsorption and Assembly of Copper Phthalocyanine on Cross- Linked TiO_2 (110)-(1 × 2) and TiO_2 (210). *J. Phys. Chem. B* **2006**, *110*, 17960–17965.
20. Matsui, M.; Akaogi, M. Molecular Dynamics Simulation of the Structural and Physical Properties of the Four Polymorphs of TiO_2. *Mol. Simul.* **1991**, *6*, 239–244.
21. Wolf, D.; Keblinski, P.; Phillpot, S. R.; Eggebrecht, J. Exact Method for the Simulation of Coulombic Systems by Spherically Truncated, Pairwise r^{-1} Summation. *J. Chem. Phys.* **1999**, *110*, 8254–8282.
22. Kulkarni, A. J.; Zhou, M.; Sarasamak, K.; Limpijumnong, S. Novel Phase Transformation in ZnO Nanowires under Tensile Loading. *Phys. Rev. Lett.* **2006**, *97*, 105502–105505.
23. Binks, D. J. Computational Modeling of Zinc Oxide and Related Oxide Ceramics. Ph.D. Thesis, University of Surrey, Harwell, 1994
24. Lin, F.; Wang, R. Systematic Derivation of AMBER Force Field Parameters Applicable to Zinc-Containing Systems. *J. Chem. Theory Comput.* **2010**, *6*, 1852–1870.
25. Singh, U. C.; Kollman, P. A. An Approach To Computing Electrostatic Charges for Molecules. *J. Comput. Chem.* **1984**, *5*, 129–145.
26. *CPMD*, V3.9; Copyright IBM Corp 1990–2001, Copyright MPI für Festkörperforshung Stuttgart 1997–2001.
27. Smith, W.; Forester, T. R. DL_POLY_2.0: A General-Purpose Parallel Molecular Dynamics Simulation Package. *J. Mol. Graphics* **1996**, *14*, 136–141.
28. Essmann, U.; Perera, L.; Berkowitz, M. L.; Darden, T.; Lee, H.; Pedersen, L. G. J. A Smooth Particle Mesh Ewald Method. *J. Chem. Phys.* **1995**, *103*, 8577–8593.
29. Bonomi, M.; Branduardi, D.; Bussi, G.; Camilloni, C.; Provasi, D.; Raiteri, P.; Donadio, D.; Marinelli, F.; Pietrucci, F.; Broglia, R.; *et al.* PLUMED: A Portable Plugin for Free-Energy Calculations with Molecular Dynamics. *Comput. Phys. Commun.* **2009**, *180*, 1961–1972.
30. Raiteri, P.; Laio, A.; Gervasio, F. L.; Micheletti, C.; Parrinello, M. Efficient Reconstruction of Complex Free Energy Landscapes by Multiple Walkers Metadynamics. *J. Phys. Chem. B* **2006**, *110*, 3533–3539.
31. Barducci, A.; Bussi, G.; Parrinello, M. Well-Tempered Metadynamics: A Smoothly Converging and Tunable Free-Energy Method. *Phys. Rev. Lett.* **2008**, *100*, 020603–020606.